Numerical Simulation of Influence of Partial Shadow on Electrical Characteristics of Photovoltaic Modules

Cheikh Ibra WADE[a)], Ryo TORIHARA[b)], Yu Mar LWIN[c)],
Tastuya SAKODA[d)], Noriyuki HAYASHI[d)]

Abstract

Influences of a partial shadow reflected on PV modules on their electrical characteristics are numerically investigated by using the LT Spice simulation and the results are discussed. Not only the change in I-V and P-V characteristics but also the change in current and voltage distribution for every cell component are demonstrated and discussed based on the numerical results. It is illustrated that the output current from a PV module is directly determined by the photo-current of the solar cell which has the lowest transmission ratio of solar irradiation under various shadow conditions, and the maximum power significantly depends on the shadow condition. It is also pointed out that the cell with the lowest transmission level among the cells concerned dominates the output characteristics of the PV module, and the diode currents concentrate to the cells which have the highest transmission level. The reverse current flows toward the modules that have a short-circuited BLDs; namely, those modules are charged from the normal modules. Those results imply the high risk of damage attributed to those reverse currents could be happened in the given PV modules. It is also indicated that the double peaks take place in the P-V characteristics, depending in the shadow transmission levels. Based on this result, it is pointed out that the voltage that corresponds to the maximum power point dynamically changes, depending on the shadow transmission levels.

Keywords: Solar power plant, Output characteristics, Partial shadow, Blocking and Bypass diodes, Numerical simulation

1. INTRODUCTION

Output power gained from a photovoltaic power plant (a PV plant) strongly depends on uncontrollable weather condition[1)]. Hence, it is important to investigate and know changes in their electrical characteristics with weather conditions[2,3)]. Today's grid-connected PV systems are frequently mounted on building roofs, facades, or generally in urban environments, where partial shading environment can frequently occur[4)]. Effects of partial shadow on PV modules are one of the important factors which provoke the change of power generation within PV system.

Wide attention has been paid with regard to predicting the behavior of output characteristics of PV systems under various shadow conditions. For example, some reports indicated that the PV module produces output current and voltage that depends on shadow's transmittance level[5, 6, 7)]. A Light-generated current increases linearly with the solar irradiation. The smaller the diode current I_D, the more current is delivered by the solar cell[8)].

This contribution shows the natures of voltage and current behavior for each devices composing the cell, as well as the whole behavior of I-V and P-V characteristics, both under different shadow conditions and under different conditions of output operation of the open-circuit, short-circuit, and maximum power point. Furthermore, the rolls of the bypass diodes and blocking diodes are demonstrated, which are obtained under various shadow conditions.

2. INFLUENCE OF PARTIAL SHADOW

2.1 Methodology

In the present simulation, a single PV module that is composed of three solar cells connected in series is employed as shown in Fig. 1. A battery that simulates the e.m.f. of the load is connected to the output terminal.

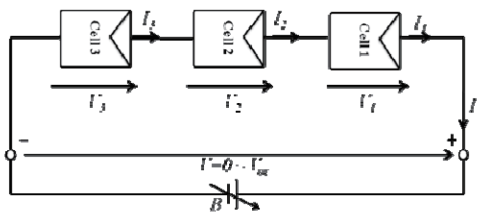

Fig. 1. A single PV module which is composed of three solar cells connected in series.

The output voltage V is given by:

$$V = V_1 + V_2 + V_3 \quad (1)$$

where V_1, V_2, and V_3 are the output voltages of Cell 1, Cell2, and Cell 3, respectively.

a) Master Student, Dept. of Electrical and Electronics Engineering
b) Doctor Student, Dept. of Materials and Informatics, Interdisciplinary Graduate School of Agriculture and Engineering (Miyazaki Prefecture Industrial Technology enter, Miyazaki)
c) Master Student, Electrical and Systems Engineering Fields
d) Professor, Dept. of Electrical and Systems Engineering

Each solar cell in the PV module is represented by a one-diode equivalent circuit shown in Fig. 2. The components in the single solar cell are a photo-current source I_{ph}, a diode D that represents the p-n junction of a solar cell, a lumped shunt resistance R_{sh}, and a lumped series resistance R_s.

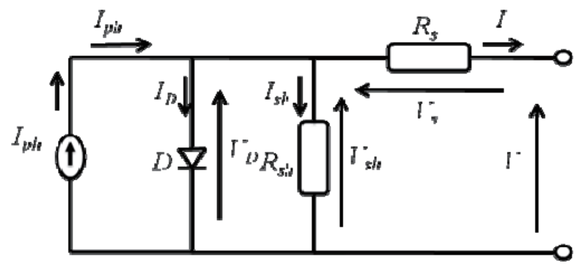

Fig. 2. Equivalent circuit of a single solar cell built in LTspice.

The current-voltage relation of a single solar cell based on this model can be written as:

$$I = I_{ph} - I_{s1}\left\{e^{\frac{qV}{n_1 kT}} - 1\right\}, \qquad (2)$$

where I is the output current of a solar cell, V the terminal voltage, I_{ph} the photo-current, I_S the reverse saturation current, q the electronic charge 1.6×10^{-19} C, n the constant of diode ideality factor, k the Boltzmann constant 1.38×10^{-23} J/K, and T the cell temperature.

Figure 3 shows the diode current I_D as a function of the diode voltage V_D; i.e., I_D-V_D characteristics of the PV cell involved in this simulation.

The LTspice IV software was used in this simulation, provided that the shunt resistance current I_{sh} was negligibly small.

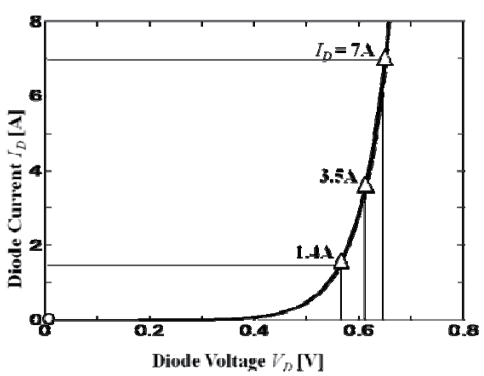

Fig.3. I_D-V_D characteristics of the diode shown in Fig. 2.

2.2 Numerical conditions

Influence of the shadow conditions on the PV module was investigated and the saturation current flowing through the diode was taken into consideration.

Two variables, α and β, are introduced to give the different level of the shadow transmission for Cell 2 and Cell 3, respectively. The transmission level of Cell 1 is set to be a unity in all cases of simulation. In this simulation, three cases of the shadow conditions were estimated as follows:

Case A) $\alpha = \beta = 1$; i.e., no shadow, resulting in uniform irradiation to all cells.

Case B) $\beta = 1$, and $\alpha < \beta$; i.e., α is the lowest shadow transmission level, resulting in partial irradiation.

Case C) $\beta < \alpha < 1$; i.e., β is the lowest shadow transmission level l, resulting in partial irradiation.

Values of photo-current I_{ph} of each cell for all cases are given in Table 1, and parameters of a solar cell used in the simulation are shown in Table 2. The value of I_S, n, R_{sh}, and R_s are derived from Ref. 9.

Table 1. Photo current of each cell.

Shadow Conditions	Photo Current I_{ph}		
	Cell 1	Cell 2	Cell 3
Case A	I_0	I_0	I_0
Case B	I_0	αI_0	I_0
Case C	I_0	αI_0	βI_0

Table 2. Parameters of a solar cell used in the simulation.

Parameter	I_{ph}	V_{oc}	I_S	n
Value	7 A	0.65 V	10^{-11} A/cm^2	1.1
Parameter	R_{sh}	R_s	T	R_{sh}
Value	10^5 Ω	10^{-4} Ω	298.15 K	10^5 Ω

2.3 Results and discussions

Numerical results obtained for I_0=7 A, α = 0.5 and β = 0.2 are demonstrated in this Section; i.e., αI_0 = 3.5 A and βI_0 = 1.4 A in Table 1. White circle (○), black circle (●) and white square (□) are used in figures hereafter so as to indicate the operation points for the short-circuit operation, the open-circuit operation, and the maximum power point (MPP) operation, respectively.

2.3.1 Output characteristics

Figure 4 shows the relationship between the output current I and voltage V obtained for the three cases. Figure 5 shows the relationship between the output power P (= V x I) and voltage V obtained for the three cases. It is clear from Figs. 4 and 5 that the I-V and P-V characteristics depend on the shadow condition to a large extent. In particular, the shadow conditions have remarkable influence on the MPP currents I_{mpp} and accordingly maximum power P_m; namely, P_m = 9.2 W (at V = 1.5 V), 5.2 W (at V = 1.6 V) and 2 W (at V = 1.62 V) for Case A, B, and C, respectively.

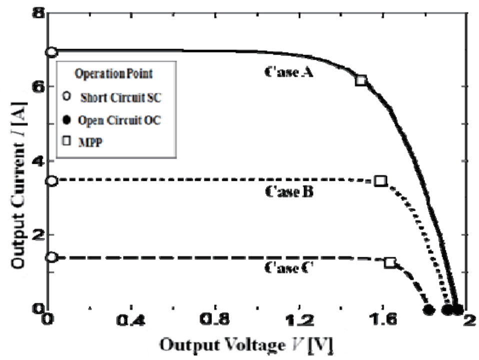

Fig. 4. P-V characteristics for three cases of shadow conditions.

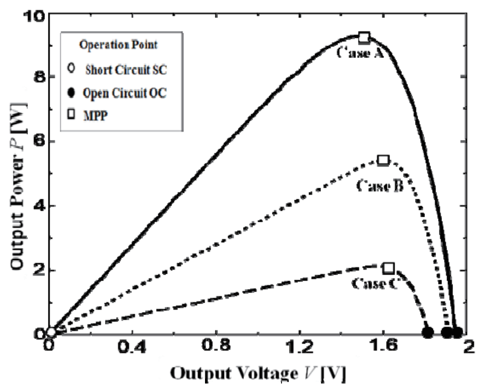

Fig. 5. P-V characteristics for three cases of shadow conditions.

2.3.2 Short-circuit current

It is clear from Fig. 4 that the shadow conditions have remarkable influence on the short-circuit currents I_{SC} of 7 A, 3.5 A and 1.4 A for Cases A, B and C, respectively, and these I_{SC} are clearly equivalent to the lowest value of I_{ph} among the three values of I_{ph} given to the three cells. Therefore, according to the numerical results, it is concluded that the short-circuit current from the module is predominantly determined by the photo-current of the cell that has the lowest transmission level under the given shadow condition.

2.3.3 Open-circuit voltage

Figures 4 and 5 indicate that the open-circuit voltage V_{OC} is also affected by the shadow conditions, and that V_{OC} decreases with the transmission level.

All amount of the photo-current of each cell flows the diode of the given cell in the open-circuit operation, and accordingly V_D of each cell can be determined by the I_D-V_D characteristics shown in Fig. 3. The white triangles in Fig. 3 indicate the data corresponding to (I_D, V_D) = (7 A, 0.65 V), (3.5 A, 0.61 V), and (1.4 A, 0.56 V).

The diode voltages of Cell 1, Cell 2, and Cell 3 (i.e., V_{D1} , V_{D2} , V_{D3}, respectively) equal to V_1, V_2, and V_3, respectively, as no voltage drop at the series resistance R_s takes place in the case of open-circuit operation, resulting in no output current. Therefore, the open circuit voltage V_{oc} can be calculated by:

$$V_{oc} = V_{D1} + V_{D2} + V_{D3} \, . \tag{3}$$

By using Eqn. (3), V_{OC} for Case A, Case B, and Case C are obtained as follows:

Case A) $V_{oc} = 0.65 + 0.65 + 0.65= 1.95$ V
Case B) $V_{oc} = 0.65 + 0.61 + 0.65= 1.91$ V
Case C) $V_{oc} = 0.65 + 0.61 + 0.56= 1.82$ V

The values of V_{oc} mentioned above reasonably agree with those shown in Figs. 4 and 5.

2.3.4 Diode voltage

The relationships between the voltage of each diode V_D and output voltage V are shown in Fig. 6 for Case B and Case C. Figure 6 indicates that the diode voltage V_D of the cell that has the lowest transmission level is negative for the lower output voltage.

2.3.5 Diode current

The relationships between the current of each diode I_D and output voltage V are shown in Fig. 7 for three Cases A, B, and C. Figure 7 indicates that the diode currents on each cell are balanced in the case of

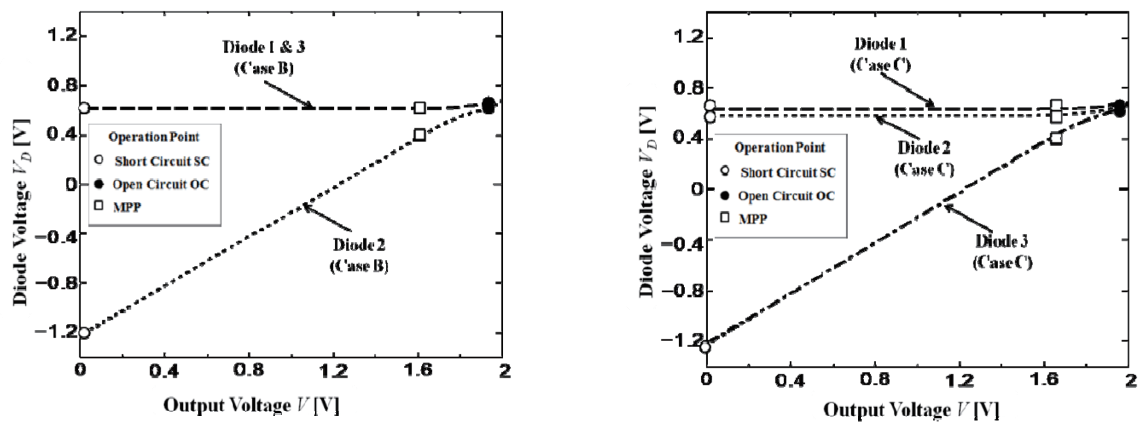

(a) Case B. (b) Case C.

Fig. 6. Relationship between the diode voltage and output voltage.

Case A, while they are significantly unbalanced in the cases of Case B and Case C. I_D of the cell on the highest transmission level is the largest among the three cells; e.g. the diode currents concentrate to the cells which have the highest transmission level.

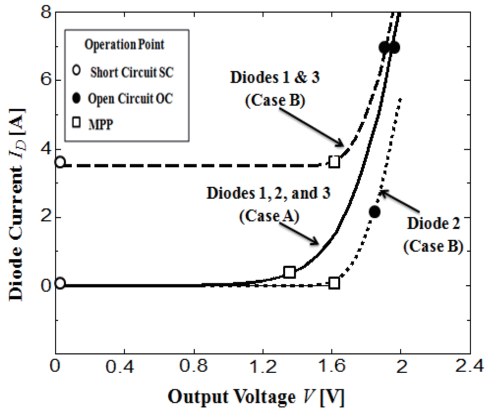

(a) In the case of Cases A and B.

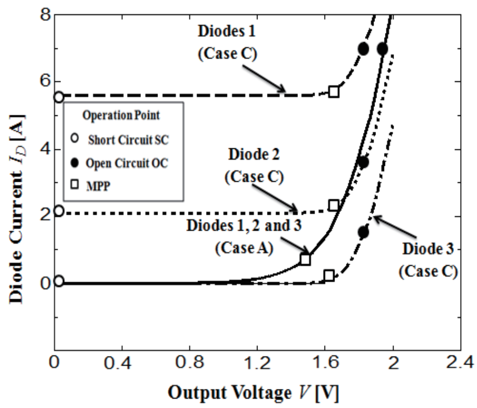

(b) In the case of Cases A and C.

Fig. 7. Relationship between the diode current and output voltage.

3. ROLLS OF BYPASS DIODES AND BLOCKING DIODES

White circle (○), black circle (●) and white square (□) are used in figures hereafter so as to indicate the operation points for the short-circuit operation, the open-circuit operation, and the maximum power point (MPP) operation, respectively.

3.1 Roll of bypass diodes

In this part of the simulation, a PV module composed of three clusters that have the bypass diodes (BPD_1, BPD_2, and BPD_3) is shown in Fig. 8, and employed in order to demonstrate the rolls of bypass diodes.

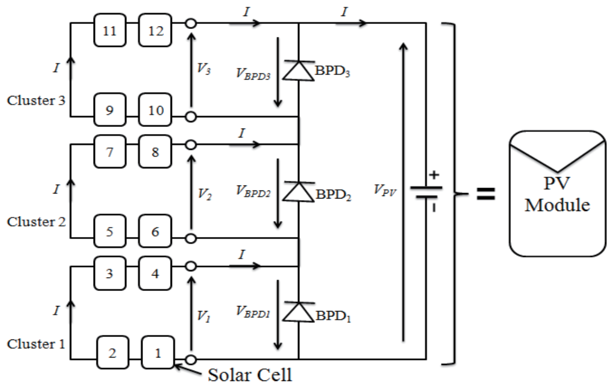

Fig. 8. A PV module employed in the simulation.

Three cases of shadow conditions were estimated as follows:

Case A) No shadow, resulting in uniform irradiation to all cells.

Case B) A single solar cell in the Cluster 1 is completely shaded.

Case C) A single solar cell of each cluster in the two Clusters 1 and 2 are completely shaded.

Figures 9 shows the I-V characteristics and P-V characteristics obtained for Cases A, B, and C. It is obvious from Fig. 9 that no current flows under Cases B and C if no BPDs is installed in the PV module. However, the installation of BPDs results in the

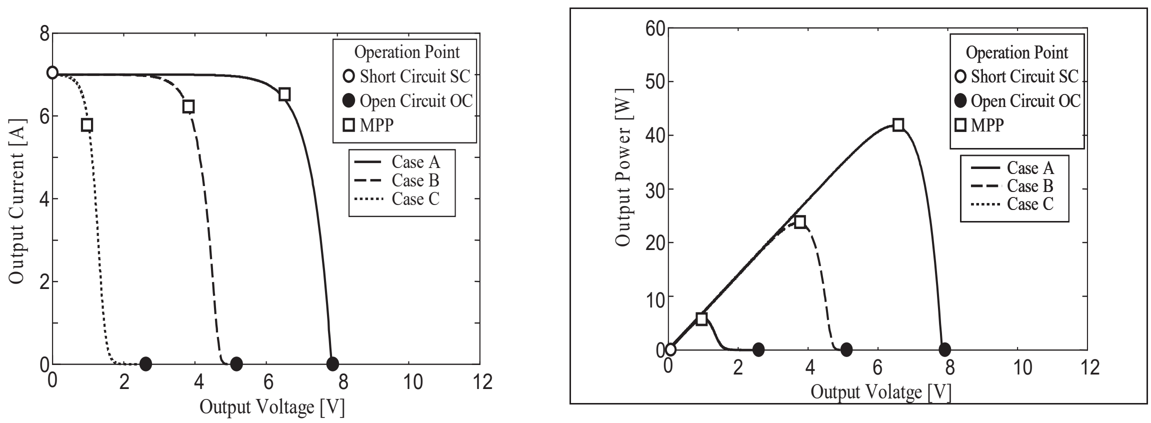

(a) I-V characteristics. (b) P-V characteristics.

Fig. 9 Advantage of the bypass diodes under various shadow conditions.

drop-out of the cluster(s) that has(have) the shaded cell(s), and the output from the rest cluster(s) is hold.

3.2 Roll of blocking diodes

A PV array composed of three PV modules that are connected in parallel across the blocking diode (BLD_1, BLD_2 and BLD_3) is shown in Fig. 10, and employed in this simulation in order to investigate the advantage and disadvantage of the blocking diode. The PV modules shown in Fig. 8 are used in this array. Here, the output current I is given by a summation of all module currents (I_1, I_2 and I_3) as follows:

$$I = I_1 + I_2 + I_3 \tag{4}$$

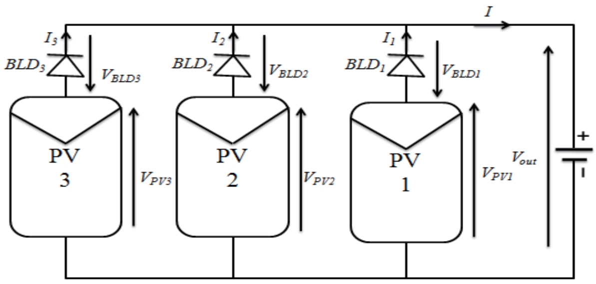

Fig. 10. A PV array employed in the simulation.

Three cases of shadow conditions were estimated as follows:

Case D) No shadow, resulting in uniform irradiation to all cells.

Case E) A single Module 3 is completely shaded.

Case F) Two Modules 2 and 3 is completely shaded.

The blocking diodes are usually installed to prevent the reverse current flow (i.e., charging of a cell) toward the cluster in the case that, under a certain circumstance, an unbalance of output voltages between the clusters takes place. For example, Fig.11 shows the current flows from/to each module (module current), which are obtained under the shadow conditions of Cases E and F. It is clearly shown in Fig. 11 that the current of the shaded module is equals to zero for both Cases E and F; namely, $I_3 = 0$ for Case E, and $I_2 = 0$ and $I_3 = 0$ for Case F, and hence no reverse current flows toward the given module.

On the other hand, Fig. 12 shows the modules currents as a function of the output voltage when the blocking diodes are short-circuited under a certain reason, which are obtained under the shadow conditions of Cases E and F. It is clearly demonstrated in Fig. 12 that the negative current flows through the module that has a short-circuited BLD is; namely,

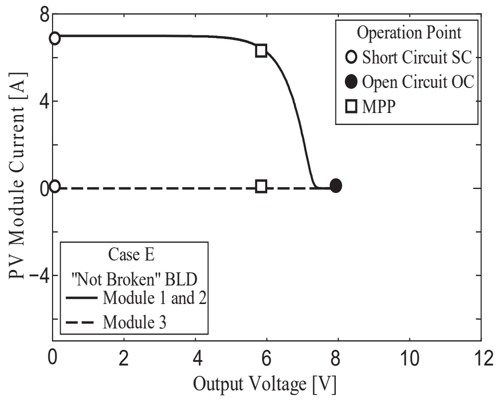

(a) Case E.

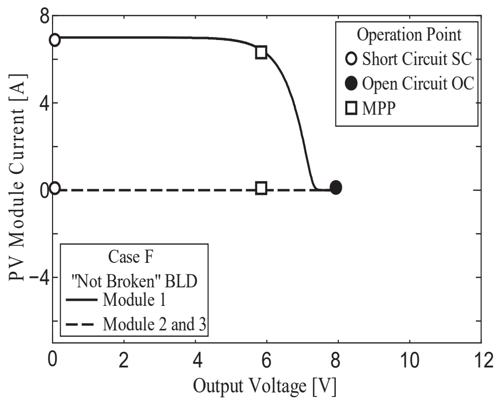

(b) Case F.

Fig. 11. Module currents under diffferent shadow conditios when all BLDs are under normal operation.

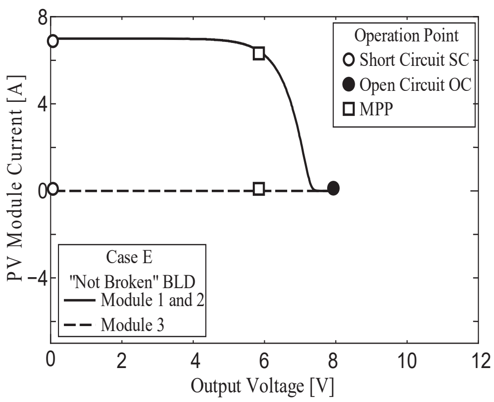

(a) Case E.

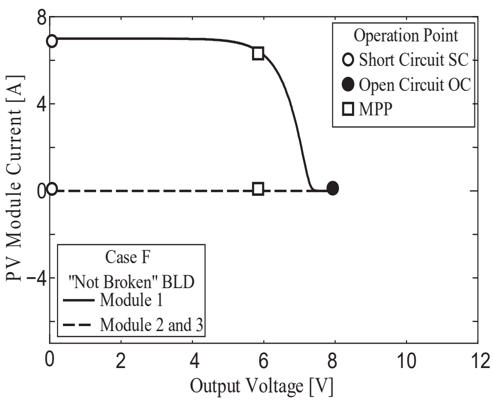

(b) Case F.

Fig. 12. Module currents under diffferent shadow conditios when all BLDs are under normal operation.

those module(s) is(are) charged from the normal module. Those results imply the existence of high risk of damage attributed to those reverse currents could be happened in the given PV modules.

4. INFLUENCE OF SHADOW TRANSMISSION LEVEL

Figure 13 shows the I-V characteristics and P-V characteristics obtained under various transmission levels of 100%, 80%, 50%, 20 and 0%, when one of the solar cells in Fig.8 (i.e., no.3 in the cluster 1) is shaded. It is obvious from Fig. 13(b) that the double peaks take place in the P-V characteristics when the shadow transmission level is between 20 to 80 %. The peak on the left-hand side is fixed to be constant, while the peak on the right-hand side decreases with the shadow transmission level. This result clearly points out that the voltage that corresponds to the maximum power point dynamically changes, depending on the shadow transmission level.

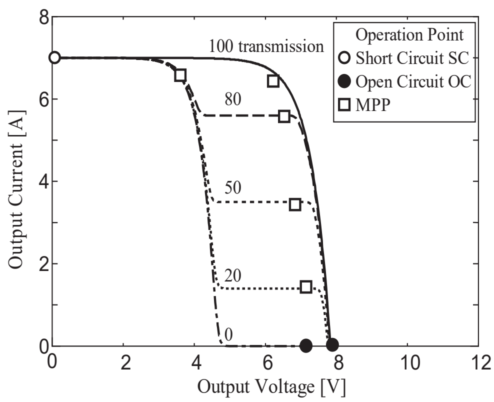

(a) I-V characteristics.

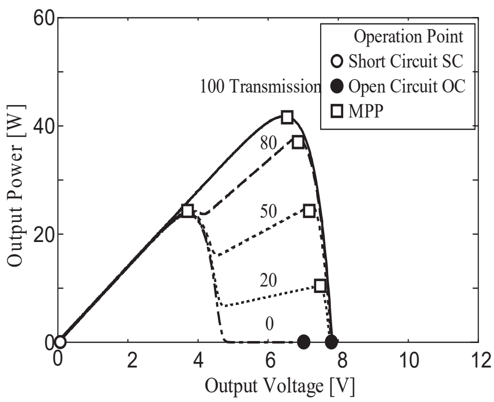

(b) P-V characteristics.

Fig. 13. Influence of transmission levels of shade.

5. CONCLUSION

The numerical results obtained from the current numerical analysis can be summarized as follows:

1) The output current from a PV module is directly determined by the photo-current of the solar cell which has the lowest transmission ratio of solar irradiation under various shadow conditions, and accordingly, the maximum power significantly depends on the shadow condition.
2) The diode currents on each cell are balanced in case of the uniform irradiation to all cells, while they are significantly unbalanced in case of non-uniform irradiation to the cells.
3) The cell with the lowest transmission level among the cells concerned dominates the output characteristics of the PV module, and the diode currents concentrate to the cells which have the highest transmission level.
4) The reverse current flows toward the modules that have a short-circuited BLDs; namely, those modules are charged from the normal modules. Those results imply the high risk of damage attributed to those reverse currents could be happened in the given PV modules.
5) The double peaks take place in the P-V characteristics when the shadow transmission level is between 20 to 80 %. Based on this result, it is pointed out that the voltage that corresponds to the maximum power point dynamically changes, depending on the shadow transmission level.

REFERENCES

1) M. C. Di Piazza and G. Vitale: Photovoltaic Source Modeling and Emulation, Springer-Verlag London 2013.
2) W. Wang, A. C-F. Liu, H. S-H. Chung, R. W-H. Lan, J. Zhang: Fault Diagnosis of Photovoltaic Panels Using Dynamic Current Voltage Characteristics, IEEE 0885-8993, 2015.
3) S. Spataru, D. Sera, T. Kerekes, R. Teodorescu: Diagnosis Method for Photovoltaic Systems Based on Light I-V measurements", Elsevier Ltd, 2015.
4) S. Guo, T. M. Walsh, A. G. Aberle and M. Peters: Analyzing Partial Shading of PV Modules by Circuit Modeling, IEEE explore 978-1-4673-0066-7/12, pp002957, 2011.
5) H. Kawamura, K. Naka, N. Yonekura, S. Yamanaka, H. Kawamura, H. Ohno and K. Naito: Simulation of I-V characteristics of a PV module with shaded PV cells, Solar Energy Materials & Solar Cells 75, 2003.
6) V. Quaschning, R. Hanitsch, "Numerical Simulation of Current Voltage Characteristics of Photovoltaic Systems with Shaded Solar Cells", Elsevier Science Ltd, Great Britain 1996.
7) E. Diaz-Dorado, A. Suarez-Garcia, C. Carrillo, J. Cidras: Influence of the Shadows in Photovoltaic Systems with Different Configuration of Bypass Diodes, IEEE, 2010.
8) H. Braun, T. Takehara, S. T. Bulddha, T. Yeider, V. Krishnan, M. Banavar, C. Tepedelenlioglu, S. Takada and A. Spanias: Signal Processing for Solar Array Monitoring, Fault Detection, and Optimization, Morgane & Claypool, 2012.
9) L. Castaner and S. Silvester: Modeling Photovoltaic Systems Using PSpice, John Wiley & Sons Ltd, England, 2002.